14.5

SURFACE ANALYSIS OF THE REAR-FLANK DOWNDRAFT IN TWO TORANDIC SUPERCELLS

Brian D. Hirth*, John L. Schroeder, and Christopher C. Weiss
Texas Tech University, Lubbock, Texas

1. INTRODUCTION

Four "mobile mesonet" instrumented vehicles, modeled after those designed by Straka et al. (1996), were used by the Texas Tech University (TTU) Atmospheric Science and Wind Science and Engineering groups to collect data during the Wheeled Investigation of Rear-flank Downdraft Lifecycles (WIRL) project in May and June of 2004 and 2005. The objective of this project was to document the evolution of RFDs in an attempt to capture the spatial and temporal changes in surface thermodymancis and kinematics and relate these changes to ongoing tornadic activity. Project WIRL provided two excellent RFD samples, the first from the 12 June 2004 supercell located west of Lehigh, IA and the second from the 9 June 2005 supercell that traversed south of Hill City, KS. These samples offer unique, high resolution data from the RFD of two tornadic supercells, which will be compared to past findings.

2. DATA COLLECTION AND ANALYSIS

Mobile mesonet (MM) data were collected at 0.5 Hz and were transferred to an on-board laptop computer running LabVIEW software for real-time display. To ensure instrument consistency between the four MM probes, vehicle intercomparisons were conducted traveling together in quiescent conditions. Offsets for each vehicle were computed relative to an overall team mean to remove any individual instrument biases. Data presented herein were constructed from 10-second averages.

Ground-relative velocity data were derived by subtracting the GPS vehicle velocity from the measured wind velocity. Due to erroneous measurements made by the flux gate compass as a result of RF noise, it was removed from the instrumentation suite. An algorithm was developed to maintain vehicle heading once vehicle speed dropped below 2.57 m s^{-1}, to account for GPS drift. Accurate wind data could then be collected while a probe was stationary and care was taken to ensure that probes maintained their heading while decelerating to a stop. Wind velocity and pressure measurements influenced by sharp changes in either speed or heading were discarded from analysis. Equivalent potential temperature (θ_e) and virtual potential temperature (θ_v) were calculated using the methods outlined by Markowski et al. (2002) and are subject to the same assumptions.

Two primary data collection routines were utilized during WIRL based on the character of the storm and the available road network and conditions. The *lifecycle* routine was executed upon intercept of a slow moving supercell located within an adequate road network allowing for continuous, mobile data acquision. In this routine, three MM probes were to orient themselves such that the western, southern, and eastern portions of the RFD were simultaneously and continuously sampled as the mesocyclone progressed in space and time. The fourth MM probe sampled the inflow environment allowing for direct thermodynamic comparisons between the various RFD sectors and the inflow "base state" (Figure 1a). Desired probe spacing was one to two kilometers within the RFD and the inflow probe was to remain several kilometers away from the main updraft yet within communication range. Individual probes remained within the RFD as long as conditions permitted with a maintained visual perspective of the low-level mesocyclone

In many cases during project WIRL, rapid storm motion, poor road networks, and unpaved road surface conditions precluded a successful attempt of the lifecycle routine leading to the development of the *snapshot* routine. Probes were positioned along a single road allowing the RFD to pass directly overhead (Figure 1b). Again, probe spacing of one to two kilometers was desired as well as the residence of one MM team in the ambient inflow environment if possible. Upon conclusion of a single snapshot sample, probes repositioned themselves upstream of the storm to repeat data acquisition.

Time-to-space conversion analysis was made possible when using the snapshot routine. Using a subjectively determined storm motion, 10-second averaged time-series data from each probe could be transformed into the spatial domain. For the case herein, storm motion was derived using the tornadogenesis time (determined by video), tornado dissipation time (determined by the National Weather Service), and the assumption of constant tornado motion. Data were then interpolated and gridded to create a two-dimensional field about the MM team array utilizing the Barnes weighting scheme. Because the resolution of data points in the east-west (x) dimension (determined by storm motion and MM

Corresponding Author Address: Brian Hirth, Texas Tech University Atmospheric Science Group, Lubbock, TX 79409-2101
brian.hirth@ttu.edu

sampling rate) was an order of magnitude higher than the north-south (y) dimension (determined by vehicle spacing) of the team array a rectangular filter (as opposed to a circle of influence) was utilized in data interpolation.

3. CASE ANALYSIS

3.1 Case 1: Lehigh, Iowa – 12 June 2004

The 11 June surface pattern was highlighted by an eastward-developing low pressure center and associated warm front in southern Minnesota/ and northern Iowa, along with a pronounced dryline in western Iowa (Figure 2). Moving southward along developing dryline convection, WIRL targeted the southernmost storm near Burnside, IA which posessed a low-level mesocyclone by 0020 UTC on 12 June. The decision was made to execute the *lifecycle* data collection routine due to an optimal local road network and slow storm motion (from 260° at 7 m s^{-1}). Probe T3 positioned west, T2 south, and T4 southeast of the low-level circulation, with probe T5 remaining further east in the inflow environment (Figure 3). The storm produced one weak, 20-minute long tornado at 0022 UTC. Multiple vortex structure was noted and damage was sustained to at least one farmstead.

T2 entered the RFD first at 0024 UTC, followed by T3 and T4. Initial θ_e deficits within the RFD were only 2 – 3 K over the first several minutes of residence (Figure 4a).[1] Heavy rain and hail began to propagate through the RFD immediately thereafter. T3 was the first to experience precipitation at 0025 UTC which was accompanied by a θ_e deficit of approximately 7 K. A more continuous decline in θ_e followed with deficits reaching 8 – 10 K relative to the measured inflow and neared 20 K by the end of the sample. T2 experienced precipitation at 0028 UTC and saw the same θ_e deficits until returning to the inflow environment around 0038 UTC. T4 received light rain starting at 0032 UTC and small hail between 0036 – 0039 UTC. Slightly warmer θ_e values were measured immediately after the start of hail fall. θ_e deficits then decreased to greater than 5 K afterwards suggesting that colder θ_e parcels of higher altitude origin were entering the RFD through precipitation drag.

Until the onset of precipitation, θ_v deficits experienced by all teams were less than 1 K. These deficits decreased with time to 3 – 4 K as the heaviest precipitation was encountered (Figure 4b). T3 experienced the greatest deficit, followed by T2 and then T4. Of note is the correlation of deficit to probe position relative to the mesocyclone and the associated duration of precipitation experienced within their respective sector of the RFD. These θ_v deficits throughout the RFD suggest that some evaporative cooling was occurring and, with simultaneous θ_e deficits, imply that RFD parcels were originating from progressively higher levels and/or were entraining environmental air consisting of colder θ_e parcels. Markowski (2002) and Markowski et al. (2002) defined "warm" ("cold") RFDs as those composed of parcels possessing small (large) θ_e and θ_v deficits compared to the storm-relative inflow, implying parcels obtained positive (negative) buoyancy. Warm (cold) RFDs were then associated with tornadogenesis (tornadogenesis falilure). It is shown that surface parcels through much of this RFD exhibited "cold" θ_e with θ_v that delimited the warm/cold threshold while maintaining a tornadic circulation. This storm was able to maintain a tornadic circulation for 20 minutes despite the adverse θ_e and threshold θ_v deficits. The overall decrease in parcel buoyancy at the surface likely led to a decrease in surface convergence under the updraft, resulting in a weak tornadic circulation as demonstrated by Markowski et al. (2003).

Overall wind speeds were relatively weak within the RFD (Figure 5). Measurements around 8 m s^{-1} were observed by all teams within the first minutes of the RFD encounter. A small-scale increase in the wind speed of T2 from 5 m s^{-1} to 12 m s^{-1} occurred between 0025 UTC and 0027 UTC, peaking near 14 m s^{-1}. Wind direction backed 50° through this feature from near 300° to 250° followed by a return back to 300°. Perhaps this maximum was related to a smaller surge within the RFD. T4 was on the inflow side of the RFD boundary at this time and could not document any potential progression of this feature. T3 recorded a relative peak in wind speed (8 m s^{-1}) from about 250° between 0024 UTC and 0025 UTC prior to a shift to 300°, similar to T2 but it is difficult to determine if this peak was associated with the same feature. In the inflow, T5 experienced a gradual backing in wind direction from 0025 to 0031 UTC along with an increase in wind speed to 12 m s^{-1}. The storm environment may have been the cause, forcing a response to increased pressure falls associated with the tornadic circulation.

3.2 Case 2: Hill City, Kansas – 9 June 2005

A surface outflow boundary producing easterly surface winds in excess of 30 kts highlighted a prolific tornadic setup on 9 June. Storm initiation on the dryline in western Kansas and potential interaction with this outflow boundary provided a target for WIRL operations (Figure 6). A storm that had initiated on the dryline south of the outflow boundary quickly organized and was isolated to the south of all other convective development. WIRL intercepted this storm 20 km southwest of Hill City around 2100 UTC. Tornadogenesis occurred at 2122 UTC, and though the interaction of a storm with pre-existing vorticity

[1] The upward plateau in θ_e measured by T4 from 0027 UTC until 0032 UTC was a result of crossing back into the inflow temporarily.

is beyond the scope of this study, interaction with the outflow boundary is strongly believed to have played a vital role in tornado production (Markowski et al. 1998, Rasumussen et al. 2000). Since Highway 283 was the only paved road option in the area, the decision was made to execute a north-south *snapshot* deployment of the RFD in advance of the storm as it propagated northeastward (Figure 7). Probe T2 was unable to remain in the inflow environment and contributed to the linear probe array within the RFD. A nearly stationary sample was made by all probes in the approximate positions of Figure 7a until the tornadic circulation was approximately 5 km east of U.S. Highway 283.

Figure 8a shows a time-to-space conversion of θ_e data collected by all probes between 2130:24 – 2141:45 UTC. The location of the tornado is centered on the origin. Inflow θ_e before encountering the RFD boundary was 354 K for all probes. All probes experienced precipitation through the period making up this analysis but T5 and T4 reported the heaviest rain and were the only two probes to see hail fall beginning just prior to the passage of the tornado. It is clear that several transient features existed prior to the passage of the circulation north of the array. θ_e values in multiple locations were greater than 3 K warmer than that found in the inflow. The source of these warmer parcels is unknown based on surface measurements alone, but their existence demonstrates multiple pockets of very buoyant parcels within the RFD upstream of the tornado. Supercell schematics (Brandes 1978, Lemon and Doswell 1979) suggest these buoyant parcels are favorably located for ingestion by the tornadic circulation and updraft. Another striking feature exists at 200,-3500 (x,y; Figure 8a). Another pocket of very buoyant surface parcels was sampled by T5 and T4. Strong wind magnitudes (>35 m s^{-1}) associated with the tornadic circulation center passing immediately to the north were measured in this region with an instantaneous value of 42 m s^{-1} by T5 (not shown). Wind direction exhibited a sharp change from westerly to easterly simultaneously. This smaller scale feature is the subject of ongoing work and is beyond the general scope of this study. The collocation of this feature with the peak wind magnitude and closest point of the array to the tornado is compelling and raises the unanswerable question: How extensive and warm were θ_e values *surrounding* the entire circulation, and what direct effect does this increased parcel buoyancy have on tornado maintenance? Further, a sharp θ_e gradient of nearly 10 K/ 2 km existed with multiple pockets of colder θ_e air to the south of this feature. As the circulation passed the array, more uniform and cold θ_e parcels were seen until, again, another pronounced pocket of warm θ_e air accompanied by stronger wind magnitudes was found amidst very heavy precipitation downstream of the circulation. This further reinforces that the θ_e makeup of surface parcels within this RFD was quite transient and spatially inconsistent throughout.

θ_v displayed a more behaved evolution as can been seen as one progresses across the RFD (Figure 8b). An inflow value of 311.5 K was measured by all probes prior to the passage of the RFD boundary and again shows that the upstream portion of the RFD contained relatively buoyant parcels. It is not until the passage of the tornado that more significant deficits on the order of 5 K were found. Once the circulation passed the array, the closer a probe was to the circulation, the colder its θ_v measurement was. It is clear by both plots in Figure 9 that parcel θ_e and θ_v can act completely independent of each other and vary significantly on small spatial scales.

4. CONCLUSIONS

Conducted during the late spring of 2004 and 2005, Project WIRL utilized four MM probes to collect high-resolution surface data within RFDs from two tornadic cases: 12 June 2004 near Lehigh, IA (Case 1) and 9 June 2005 near Hill City, KS (Case 2). Using different data collection techniques, each case provides its own perspective of a tornadic RFD.

Case 1 offered contradiction to the summary of cases in Markowski et al. (2002) where a sustained tornado existed despite especially "cold" θ_e perturbations and "threshold" θ_v perturbations within the RFD. This particular RFD was also associated with relatively weak surface winds, especially prior to the onset of precipitation.

The supercell in Case 2 became rooted along a surface baroclinic (outflow) boundary producing a large, long-track tornado. θ_e and θ_v deficits were generally less than 4 K until after the circulations passage and precipitation inundated the entire downdraft. Several transient θ_e pockets could be seen throughout the RFD, while θ_v remained relatively well behaved. Even with the presence of significant precipitation and hail within the RFD, θ_v deficits remained generally less than 5 K for all teams through the entire sampling period, consistent with the findings of Markowski et al. (2002).

The spatial variations in parcel buoyancy found in these cases show that multiple RFD forcings are acting at any given time during the life of an RFD. Further, thermodynamic conditions that would intuitively leave one to believe negative buoyancy exists near a tornado (e.g., heavy precipitation, hail) may be offset by separate mechanisms transporting more buoyant parcels to the surface (e.g., non-hydrostatic pressure perturbations). These findings show that a RFD can be comprised of parcels of significantly varying origin and composition.

Acknowledgements

Funding was provided by the NSF Grant IGERT-0221688 and the Department of Commerce NIST/Texas Tech University Cooperative Agreement Award 70NANB8H0059. We thank all those who volunteered in the field and particular thanks are extended to Ian Giammanco for his time spent with MM and communication preparations.

5. REFERENCES

Brandes, E. A., 1978: Mesocyclone evolution and tornadogenesis: Some observations. *Mon. Wea. Rev.*, 106, 995-1011.

Lemon, L. R., and C. A. Doswell, 1979: Severe thunderstorm evolution and mesocylone structure as related to tornadogenesis. *Mon. Wea. Rev.*, **107**, 1184-1197.

Markowski, P. M., 2002: Mobile mesonet observations on 3 May 1999. *Weather and Forecasting*, **17,** 430-444.

_____, E. N. Rasmussen, and J. M Straka, 1998: The occurrence of tornadoes in supercells interacting with boundaries during VORTEX-95. *Wea. Forecasting*, **13,** 852-859.

_____, J. M. Straka, and E. N. Rasmussen, 2002: Direct thermodynamic observations within the rear-flank downdraft of nontornadic and tornadic supercells. *Mon. Wea. Rev.*, **130,** 1692-1721.

_____, _____, and _____, 2003: Tornadogenesis resulting from the transport of circulation by a downdraft: Idealized numerical simulations. *J. Atmos. Sci.*, **60,** 795-823.

Rasmussen, E.N., J. M. Straka, R.P. Davies-Jones, C. A. Doswell, F. H. Carr, M. D. Eilts, and D. R. MacGorman, 1994: Verification of the Origins of Rotation in Tornadoes Experiment: VORTEX. *Bull. Amer. Meteor. Soc.*, **75**, 995-1006.

Straka, J. M., E. N. Rasmussen, and S. E. Fredrickson, 1996: A mobile mesonet for finescale meteorological observations. *J. Atmos. Oceanic. Technol.*, **13,** 921-936.

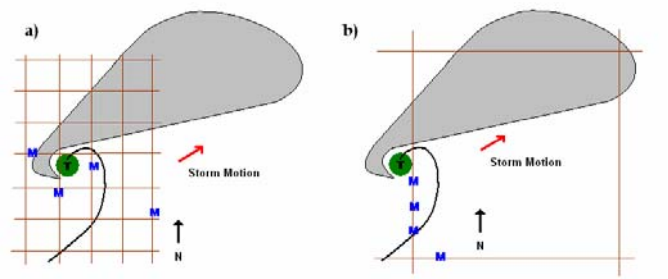

Figure 1 Schematic diagram of the (a) lifecycle and (b) snapshot data collection routines. The RFD boundary is indicated by a solid black line while individual MM teams are marked with an "M". Location of low-level mesocyclone or tornado is denoted with a "T". The storm motion vector and orientation of true north are provided. The idealized road grid spacing in (a) is approximately one kilometer by one kilometer and will vary in (b).

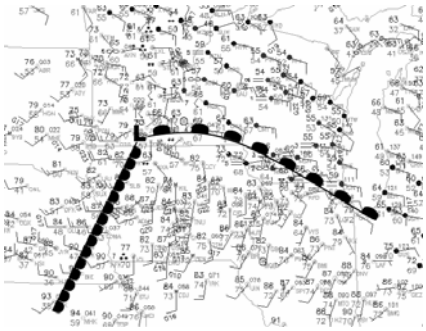

Figure 2 Subjective surface analysis from 2343 UTC on 11 June 2004. Standard synoptic symbols are used.

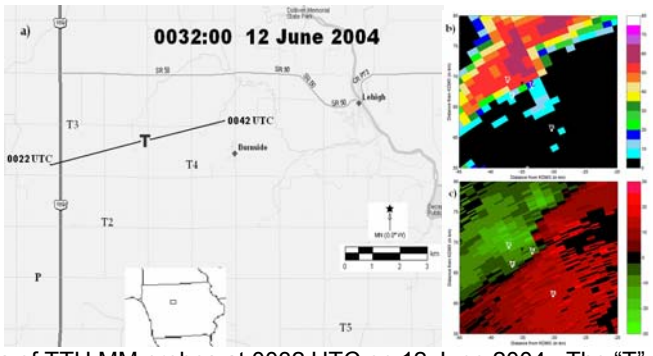

Figure 3 (a) Locations of TTU MM probes at 0032 UTC on 12 June 2004. The "T" denotes the location of the tornado on the ground at this time. The "P" indicates where all probes were located at 0022 UTC when the circulation on the ground was first noticed. The solid line indicates the path of the tornado until it was no longer visible at 0042 UTC. Locations of MM probes at 0034 UTC overlayed by the KDMX WSR-88D (b) base reflectivity and (c) base radial velocity are also shown (elevation of scan is ~650 m AGL). The black "T" represents the subjectively determined position of the tornado.

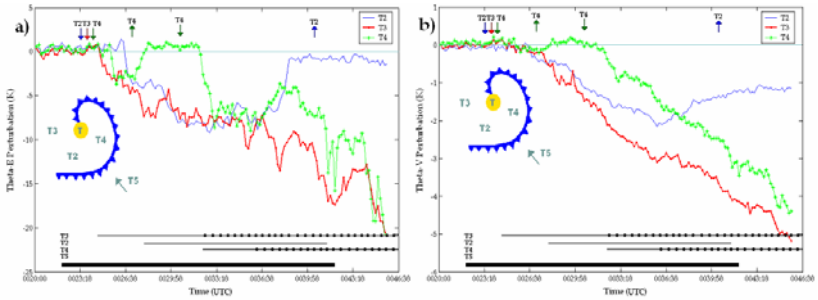

Figure 4 Time series of (a) equivalent and (b) virtual potential temperature perturbations (K) compared to that of the inflow environment (T5) during the 12 June 2004 Lehigh, IA tornadic RFD sample. The time series for T2 is denoted by a solid blue line, T3 by a bold red line with dots, and T4 by a solid green line with asterisks. A schematic of probe position during the sample is also shown. Above the time series, down arrows denote the time that individual MM probes entered the RFD from the inflow, while up arrows denote the time that individual MM probes entered the inflow environment from the RFD. The solid bars at the bottom of the plot indicate the duration of precipitation for each probe, with circles indicating hail duration, where documented. The bold bar at the bottom of the figure denotes the duration in which the tornado was on the ground *and visible*.

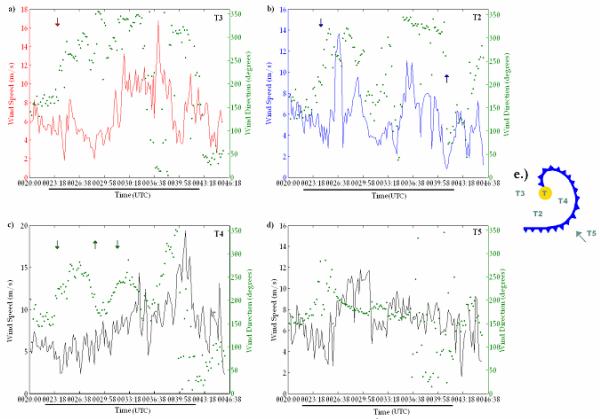

Figure 5 Plots of derived mean wind speed (solid line, m s^{-1}) and direction (dotted line, degrees) for (a) T3, (b) T2, (c) T4, and (d) T5 during the Lehigh, IA tornadic RFD sample on 12 June 2004. The horizontal bar along the bottom of each plot denotes the time during which the tornado was on the ground and visible. Downward pointing arrows indicate when each probe member entered the RFD while upward pointing arrows indicate when each probe exited the RFD, where applicable. A schematic of general car positions (e) is also shown for reference.

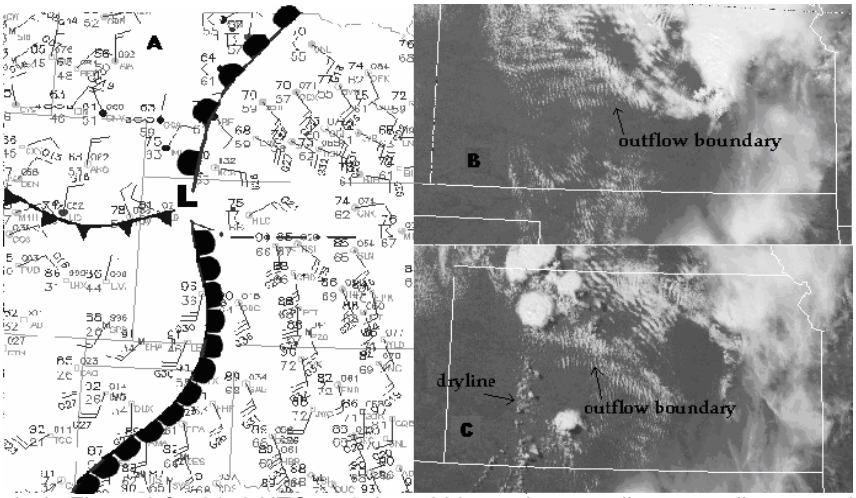

Figure 6 (a) As in Figure 3 for 2143 UTC on 9 June 2005 as the tornadic supercell was south/southeast of Hill City. The outflow boundary is described by a dot-dash line. Visible satellite imagery from 9 June 2005 is also shown at (b) 1825 UTC and (c) 2010 UTC.

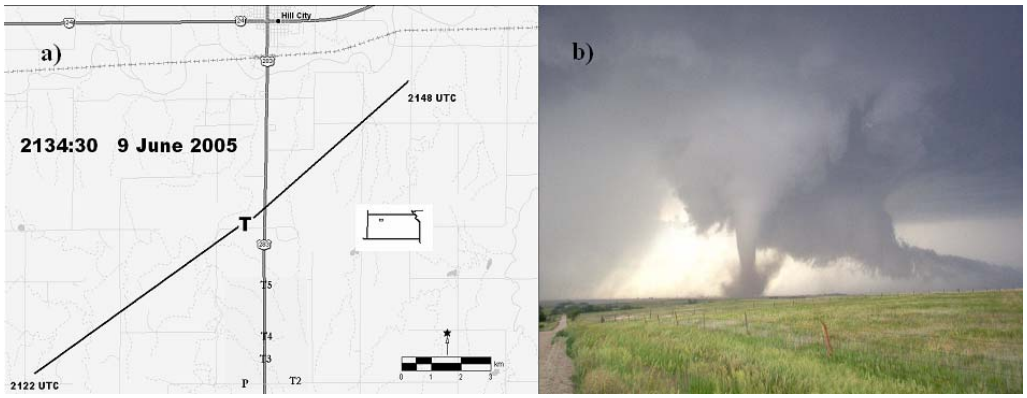

Figure 7 (a) Locations of the four TTU MM probes at 2134:30 UTC. The "T" denotes the location of the tornado on the ground at this time. The "P" indicates where all probes were located at 2122 UTC when the circulation on the ground was first noticed. The solid line indicates the path of the tornado until it was no longer visible at 2140 UTC. An photograph of the tornado at 2125 UTC 20 km southwest of Hill City, KS is shown in (b). Photo taken by Eric Thoen.

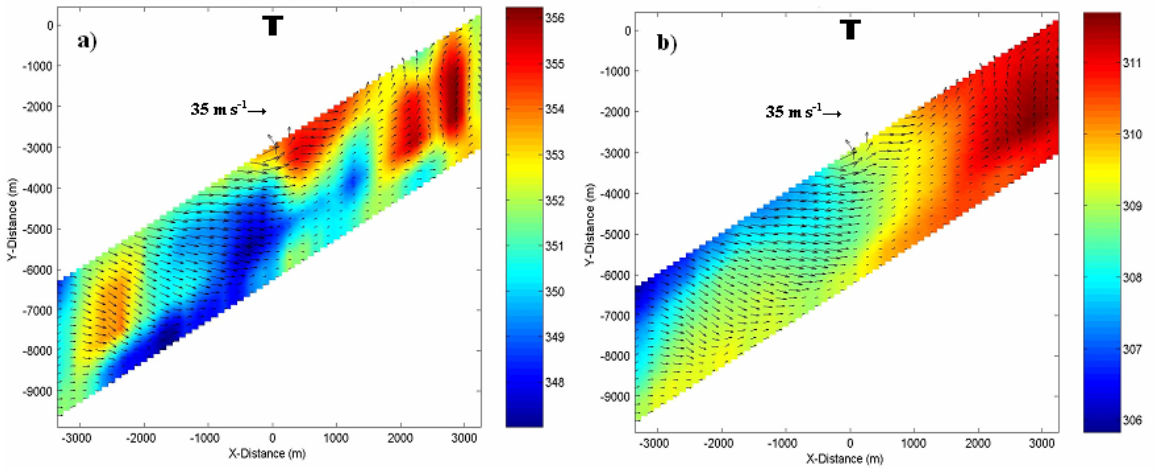

Figure 8 Time to space conversion of (a) equivalent and (b) virtual potential temperature (K) during the 9 June 2005 Hill City, KS tornadic RFD sample. The data presented spans from 2130:24 UTC to 2141:45 UTC. Derived wind vectors are overlayed. The "T" at the origin represents the location of the tornado.